

# Van der Waals heterostructures

A. K. Geim<sup>1,2</sup> & I. V. Grigorieva<sup>1</sup>

Research on graphene and other two-dimensional atomic crystals is intense and is likely to remain one of the leading topics in condensed matter physics and materials science for many years. Looking beyond this field, isolated atomic planes can also be reassembled into designer heterostructures made layer by layer in a precisely chosen sequence. The first, already remarkably complex, such heterostructures (often referred to as ‘van der Waals’) have recently been fabricated and investigated, revealing unusual properties and new phenomena. Here we review this emerging research area and identify possible future directions. With steady improvement in fabrication techniques and using graphene’s springboard, van der Waals heterostructures should develop into a large field of their own.

Graphene research has evolved into a vast field with approximately ten thousand papers now being published every year on a wide range of graphene-related topics. Each topic is covered by many reviews. It is probably fair to say that research on ‘simple graphene’ has already passed its zenith. Indeed, the focus has shifted from studying graphene itself to the use of the material in applications<sup>1</sup> and as a versatile platform for investigation of various phenomena. Nonetheless, the fundamental science of graphene remains far from being exhausted (especially in terms of many-body physics) and, as the quality of graphene devices continues to improve<sup>2–5</sup>, more breakthroughs are expected, although at a slower pace.

Because most of the ‘low-hanging graphene fruits’ have already been harvested, researchers have now started paying more attention to other two-dimensional (2D) atomic crystals<sup>6</sup> such as isolated monolayers and few-layer crystals of hexagonal boron nitride (hBN), molybdenum disulphide (MoS<sub>2</sub>), other dichalcogenides and layered oxides. During the first five years of the graphene boom, there appeared only a few

experimental papers on 2D crystals other than graphene, whereas the last two years have already seen many reviews (for example, refs 7–11). This research promises to reach the same intensity as that on graphene, especially if the electronic quality of 2D crystals such as MoS<sub>2</sub> (refs 12, 13) can be improved by a factor of ten to a hundred.

In parallel with the efforts on graphene-like materials, another research field has recently emerged and has been gaining strength over the past two years. It deals with heterostructures and devices made by stacking different 2D crystals on top of each other. The basic principle is simple: take, for example, a monolayer, put it on top of another monolayer or few-layer crystal, add another 2D crystal and so on. The resulting stack represents an artificial material assembled in a chosen sequence—as in building with Lego—with blocks defined with one-atomic-plane precision (Fig. 1). Strong covalent bonds provide in-plane stability of 2D crystals, whereas relatively weak, van-der-Waals-like forces are sufficient to keep the stack together. The possibility of making multilayer van der Waals heterostructures has been demonstrated experimentally only

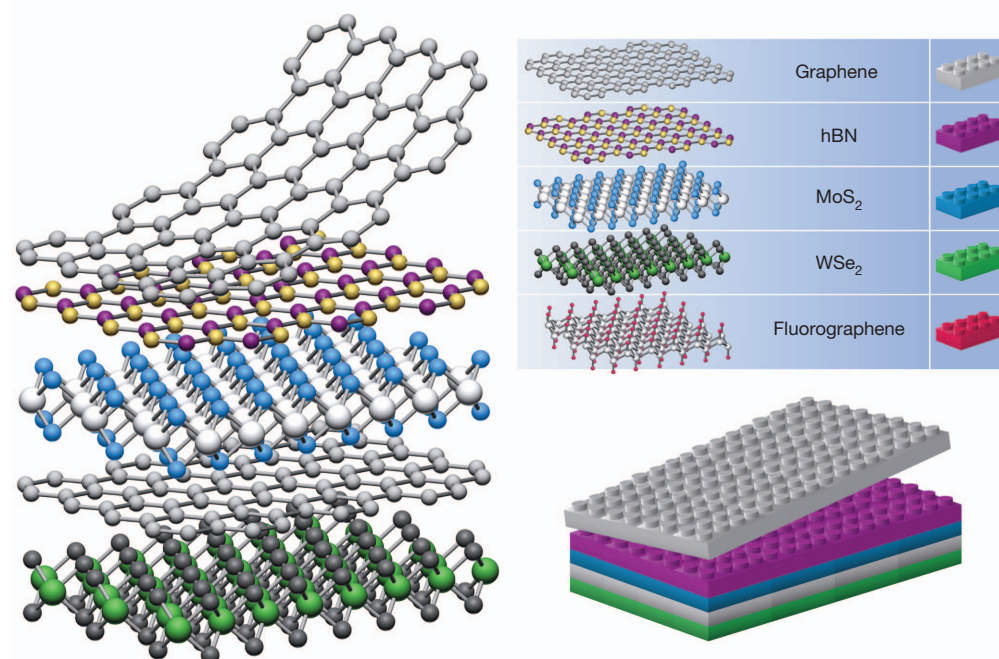


**Figure 1 | Building van der Waals heterostructures.** If one considers 2D crystals to be analogous to Lego blocks (right panel), the construction of a huge variety of layered structures becomes possible. Conceptually, this atomic-scale Lego resembles molecular beam epitaxy but employs different ‘construction’ rules and a distinct set of materials.

<sup>1</sup>School of Physics and Astronomy, University of Manchester, Manchester M13 9PL, UK. <sup>2</sup>Centre for Mesoscience and Nanotechnology, University of Manchester, Manchester M13 9PL, UK.

recently<sup>14–19</sup>. Most importantly, it turned out that in practice this atomic-scale Lego works exceptionally well, better than one could have imagined. How it works and why van der Waals heterostructures deserve attention is discussed in this Perspective.

## Dreamscape

For any research subject, it is helpful to have a big idea, even if it is unlikely to be realized in its original form. In the case of graphene, its biggest ambition has been to grow into the new silicon, offering a lifeline for Moore's law<sup>1</sup>. At the time of writing, the dreams of other 2D crystals are relatively more modest. They are often about offering alternative solutions to compensate for graphene's weaknesses<sup>7–11</sup>. In contrast, van der Waals heterostructures do not lack ambition.

Imagine the following structure. Graphene is put on top of a dielectric crystal a few layers thick (for example, mica), and the sequence is repeated again and again. The resulting van der Waals crystal is superficially similar to superconducting copper oxides, with graphene playing the part of conductive CuO planes and the 2D high- $\kappa$  dielectrics providing interplanar spacing. The critical temperature  $T_C$  of oxide superconductors depends on many materials parameters, including the CuO interlayer spacing<sup>20,21</sup>. Careful tuning of these parameters allows  $T_C$  above 130 K. However, the standard growth techniques offer limited scope for varying the parameters, and progress has stalled. What if we mimic layered superconductors by using atomic-scale Lego? Bismuth strontium calcium copper oxide superconductors (BSCCO) can be disassembled into individual atomically thin planes<sup>6</sup>. Their reassembly with some intelligently guessed differences seems worth a try, especially when the mechanism of high- $T_C$  superconductivity remains unknown. Moreover, graphene seems to be a natural choice of 2D component in the search for new layered superconductors. Indeed, intercalated graphite exhibits a respectable  $T_C$  above 10 K (ref. 22) and can be viewed as a stack of heavily doped graphene planes with an increased interlayer distance. What if a dielectric plane of, for example, BSCCO or hBN is added in between the planes of intercalated graphite? Such artificial materials engineered with one-atomic-plane accuracy would have been science fiction a few years ago but are within the grasp of today's technology.

We have used the above example for its straightforward appeal and because high- $T_C$  superconductivity in doped graphene has been widely proposed (see refs 23–26). Yet van der Waals heterostructures bring to mind not one but many similar speculative ideas. Another example is a room-temperature excitonic superfluidity suggested for two graphene layers separated by an ultrathin dielectric<sup>27,28</sup>. On the scale of such dramatic perspectives, it may sound fairly modest that van der Waals heterostructures also offer a helping hand in graphene's efforts to go beyond silicon<sup>1,15</sup>. Of course, one can think of many arguments why these or similar ideas can fail. In blue-sky research, even the most plausible scenarios often do. However, big dreams are essential to keep us trying and to serve as Ariadne's thread when exploring new topics. Having said that, it is equally important not to get lost on the way by checking grand ideas against contemporary reality.

## Layered reality check

Before explaining how to make van der Waals heterostructures, it is instructive to review the existing library of 2D crystals, those individual components that can be used in the assembly. In principle, there exist hundreds of layered materials that cleave easily, and one can naturally think of using, for example, the same Scotch-tape cleaving technique to isolate their atomic planes<sup>6</sup>. Unfortunately, this is not straightforward. One must remember that (1) melting temperature decreases with decreasing the thickness of thin films and (2) most materials survive our ambient conditions only by natural passivation of their surfaces<sup>29</sup>. Monolayers have two surfaces and no bulk in between, which presents the extreme case of surface science. On the other hand, neither of the procedures developed for isolating 2D crystals can currently be carried out in high vacuum or at low temperature, which are typical surface-science requirements. And graphene monolayers are notably more reactive than even

graphene bilayers<sup>30,31</sup>. In short, many 2D crystals imaginable in theory are unlikely to survive in reality because they would corrode, decompose, segregate and so forth<sup>29</sup>.

The high thermal and chemical stability of a three-dimensional (3D) crystal is essential before one can even contemplate the possibility of its 2D counterpart. Graphite has both, allowing graphene to exist under ambient conditions. The same is valid for other stable 2D crystals in Fig. 2. Nonetheless, the surface of MoS<sub>2</sub> starts oxidizing in moist air below 100 °C (ref. 32). Even graphene would not survive if our rooms were twice as hot, at 600 K (ref. 30). Take, for example, GaSe, TaS<sub>2</sub> or Bi<sub>2</sub>Se<sub>3</sub>. These materials are stable in bulk but, once cleaved down to a few layers, corrode. An illuminating case is silicene<sup>33,34</sup>. This 2D silicon can be grown epitaxially and investigated in high vacuum. However, it is not expected to survive isolation from its parent substrate or exposure to air. With contemporary technologies, the silicene transistors envisaged in the literature cannot be made. These examples are given to say that, because of the poor stability of atomically thin films compared to their 3D counterparts, the library of 2D crystals should be relatively limited.

Another important consideration is interfacial contamination. Adsorbates such as water, hydrocarbons and so on cover every surface, unless it is prepared under extreme surface-science conditions. Graphene is densely covered with hydrocarbons, even after annealing in the high vacuum of a transmission electron microscope. It takes considerable effort to find clean patches several nanometres in size<sup>16</sup>. (Note that this contamination is highly mobile and usually remains unnoticeable for scanning probe microscopy.) If isolated 2D crystals are stacked together, the surface contamination becomes trapped in between layers. Therefore, van der Waals heterostructures should generally be expected to become 'layer cakes' glued by contamination rather than the neat crystals imagined in Fig. 1. This scenario would remove much of the appeal from van der Waals heterostructures because it is difficult to control the manufacture and reproducibility of 'layer cakes'. Fortunately, it turns out that contamination can clean itself off the interfaces<sup>16,19,35</sup>, as further discussed below.

## Two-dimensional family values

At the time of writing, we can be certain of the existence of more than a dozen different 2D crystals under ambient conditions. First of all, these are monolayers of graphite, hBN and MoS<sub>2</sub>, which have been studied extensively. It is probably not coincidental that these materials are widely used as solid lubricants, which requires high thermal and chemical stability. There are also 2D tungsten disulphide (WS<sub>2</sub>), tungsten diselenide (WSe<sub>2</sub>) and molybdenum diselenide (MoSe<sub>2</sub>), which are chemically, structurally and electronically similar to MoS<sub>2</sub>. Despite little research having been done so far on the latter monolayers, it is safe to add them to the 2D library, too (Fig. 2).

Among the above 2D crystals, graphene is an unequivocal champion, exhibiting the highest mechanical strength and crystal and electronic quality. It is likely to be the most common component in future van der Waals heterostructures and devices. Latest developments on graphene include micrometre-scale ballistic transport at room temperature (refs 3, 36) and low-temperature carrier mobilities of  $\mu \approx 10^6 \text{ cm}^2 \text{ V}^{-1} \text{ s}^{-1}$  in suspended devices<sup>4,5</sup>. The runner-up is 2D hBN, or 'white graphene'. Its rise started when bulk hBN crystals<sup>37,38</sup> were shown to be an exceptional substrate for graphene, allowing a tenfold increase in its electronic quality<sup>2</sup>. This advance attracted immediate attention and, shortly after, few-layer crystals and monolayers of hBN were used as gate dielectrics<sup>14,39</sup> and tunnel barriers (2D hBN can sustain biases up to about  $0.8 \text{ V nm}^{-1}$  and be free from pinholes)<sup>40,41</sup>.

Monolayers of MoS<sub>2</sub> were studied earlier<sup>6,42</sup>, including the demonstration of the electric field effect, but they received little attention until devices with switching on/off ratios of  $>10^8$  and room-temperature  $\mu \approx 100 \text{ cm}^2 \text{ V}^{-1} \text{ s}^{-1}$  were reported<sup>12</sup>. Although these mobilities are much lower than in graphene, they are still remarkably high compared with thin-film semiconductors. The large on/off ratios are due to a sizeable bandgap in MoS<sub>2</sub>. It is direct in a monolayer (about 1.8 eV), whereas bilayer and few-layer MoS<sub>2</sub> are indirect bandgap semiconductors<sup>43,44</sup>.

Graphene family	Graphene	hBN 'white graphene'	BCN	Fluorographene	Graphene oxide
2D chalcogenides	MoS <sub>2</sub> , WS <sub>2</sub> , MoSe <sub>2</sub> , WSe <sub>2</sub>		Semiconducting dichalcogenides: MoTe <sub>2</sub> , WTe <sub>2</sub> , ZrS <sub>2</sub> , ZrSe <sub>2</sub> and so on	Metallic dichalcogenides: NbSe <sub>2</sub> , NbS <sub>2</sub> , TaS <sub>2</sub> , TiS <sub>2</sub> , NiSe <sub>2</sub> and so on	
				Layered semiconductors: GaSe, GaTe, InSe, Bi <sub>2</sub> Se <sub>3</sub> and so on	
2D oxides	Micas, BSCCO	MoO <sub>3</sub> , WO <sub>3</sub>	Perovskite-type: LaNb <sub>2</sub> O <sub>7</sub> , (Ca,Sr) <sub>2</sub> Nb <sub>3</sub> O <sub>10</sub> , Bi <sub>4</sub> Ti <sub>3</sub> O <sub>12</sub> , Ca <sub>2</sub> Ta <sub>2</sub> TiO <sub>10</sub> and so on	Hydroxides: Ni(OH) <sub>2</sub> , Eu(OH) <sub>2</sub> and so on	
	Layered Cu oxides	TiO <sub>2</sub> , MnO <sub>2</sub> , V <sub>2</sub> O <sub>5</sub> , TaO <sub>3</sub> , RuO <sub>2</sub> and so on		Others	

**Figure 2 | Current 2D library.** Monolayers proved to be stable under ambient conditions (room temperature in air) are shaded blue; those probably stable in air are shaded green; and those unstable in air but that may be stable in inert atmosphere are shaded pink. Grey shading indicates 3D compounds that have been successfully exfoliated down to monolayers, as is clear from atomic force microscopy, for example, but for which there is little further information. The

data given are summarized from refs 6–11, 42 and 55. We note that, after intercalation and exfoliation, the oxides and hydroxides may exhibit stoichiometry different from their 3D parents (for example, TiO<sub>2</sub> exfoliates into a stoichiometric monolayer of Ti<sub>0.87</sub>O<sub>2</sub>; ref. 8). 'Others' indicates that many other 2D crystals—including borides, carbides, nitrides and so on—have probably been<sup>7–11</sup> or can be isolated. BCN, boron carbon nitride.

Semiconductors with a direct gap are of special interest for use in optics and optoelectronics. Further interest in monolayer MoS<sub>2</sub> is due to the broken centrosymmetry that allows efficient spin and valley polarization by optical pumping<sup>45,46</sup>. This research is stimulated by the availability of large molybdenite crystals from several mining sources. The absence of such supply is probably the reason why 2D WS<sub>2</sub>, WSe<sub>2</sub> and MoSe<sub>2</sub> attract relatively little attention despite the fact that Raman and transport studies have revealed their electronic structures and quality to be similar to that of MoS<sub>2</sub> (refs 47–49). The differences between these dichalcogenides worth noting are the stronger spin–orbit coupling in the W compounds and the lower stability of the Se compounds.

There have been reports on exfoliation of many other layered chalcogenides down to a monolayer (Fig. 2). However, we have chosen only to 'pencil' them into the 2D library because little is known about their stability, let alone their optical and transport properties. In some cases, it is even unclear whether the observed flakes and suspensions are indeed 2D counterparts of the parent crystals or present different chemical entities after exposure to air or liquids. In our experience, monolayers of metallic dichalcogenides are unstable in air (T. Georgiou, R. R. Nair, A. Mishchenko, K. S. Novoselov & A.K.G., manuscript in preparation).

Another group of 2D crystals are numerous oxides including monolayers of TiO<sub>2</sub>, MoO<sub>3</sub>, WO<sub>3</sub>, mica and perovskite-like crystals such as BSCCO and Sr<sub>2</sub>Nb<sub>3</sub>O<sub>10</sub> (for reviews, see refs 7–11). As oxides, these crystals are less susceptible to air but they tend to lose oxygen and may react with minority chemicals (for example, water and hydrogen). Similarly to other atomically thin crystals, properties of 2D oxides are expected to differ from those of their parents owing to quantum confinement. Indeed, monolayer oxides often have lower dielectric constants and larger bandgaps than their 3D counterparts<sup>8</sup> and can exhibit charge density waves<sup>6</sup>. Unfortunately, information about oxide monolayers is limited mostly to their observation with atomic force and electron microscopes. The heavy artillery of physics and nanotechnology such as the electric field effect, Raman and optical spectroscopy, tunnelling, and so on have not yet been applied to isolated 2D oxides. We should also mention 2D hydroxides that can be exfoliated down to a monolayer but even less is known about them<sup>7</sup>.

Finally, there are several graphene derivatives (Fig. 2). One of them is fluorographene, a stable stoichiometric wide-gap insulator, which can be obtained by fluorination of graphene<sup>50</sup>. Unfortunately, only crystals with poor electronic quality have been reported so far. Graphane (fully hydrogenated graphene) gradually loses its hydrogen<sup>51</sup> and is unlikely to be useful for making heterostructures. Nonetheless, we note that hydrogenated or other derivatives can sometimes be more stable than 2D crystals themselves<sup>51</sup>. Finally, let us mention graphene oxide<sup>52</sup> and monolayers of boron carbon nitride<sup>53,54</sup>, which although non-stoichiometric, can also be considered for designing van der Waals heterostructures.

## Rules of survival

As interest in graphene-like crystals rapidly grows<sup>7–11</sup>, the search for new 2D candidates is expected to intensify, too. In this regard, the following rule of thumb can be helpful. First, 3D materials with melting temperature over 1,000 °C have the best chances of having 2D counterparts stable at room temperature. Second, 3D parents must be chemically inert and exhibit no decomposed surface layer in air or an alternative environment where exfoliation takes place. Third, insulating and semiconducting 2D crystals are more likely to be stable than metallic ones, owing to the generally higher reactivity of metals. In all cases, visual evaluation and Raman spectroscopy are helpful to provide a rapid test for the absence of corrosion and the presence of essential signatures indicating a similarity to the parent crystal. However, the ultimate proof lies with electrical measurements of either in-plane transport for conducting 2D crystals or out-of-plane tunnelling through insulating ones to check for their homogeneity and the absence of pinholes.

As a further step towards expanding the 2D library, one can perform isolation and encapsulation in an inert atmosphere. Many metallic 2D dichalcogenides may then remain stable at room temperature, as their stability in solvents seems to indicate<sup>55,56</sup>. This approach can also lead to higher electronic quality for present favourites such as graphene and 2D MoS<sub>2</sub>. Exfoliation-encapsulation at low temperature (such as in liquid nitrogen) is in principle possible but for the moment too difficult to contemplate for practical use. Lastly, monolayers may exist without a layered 3D parent (examples are silicene and monolayers of Y<sub>2</sub>O<sub>3</sub> and ZnO)<sup>57,58</sup>. If the monolayers are sufficiently stable, the substrate can be etched away, as demonstrated for graphene grown on metal foils<sup>59–61</sup>. This can provide access to 2D crystals without 3D layered analogues in nature.

## Lego on atomic scale

It is no longer adventurous to imagine the automated, roll-to-roll assembly<sup>61</sup> of van der Waals heterostructures using sheets of epitaxially grown 2D crystals<sup>59–63</sup>. However, concerted efforts towards such assembly are expected only when a particular heterostructure proves to be worthy of attention, as happened in the case of graphene on hBN<sup>64</sup>. For scouting which area to focus on, manual assembly is likely to remain the favourite approach. It offers high throughput and relatively easy changes in layer sequences. Likewise, individual 2D compounds will continue to be obtained by the Scotch-tape technique, which has so far provided crystallites of unmatched quality. Nevertheless, we expect the increasingly frequent use of epitaxially grown graphene, 2D hBN, 2D MoS<sub>2</sub>, and so on for making proof-of-concept van der Waals heterostructures.

At the time of writing, only a few groups have reported van der Waals heterostructures made from more than two atomically thin crystals, and only graphene and few-layer hBN, MoS<sub>2</sub> and WS<sub>2</sub> were used for this



assembly<sup>14–19,65,66</sup>. A typical stacking procedure starts by isolating micro-metre-sized 2D crystals on top of a thin transparent film (for example, polymer). The resulting 2D crystal provides one brick for the Lego wall in Fig. 1 and can now be put face down onto a chosen target. The supporting film is then removed or dissolved. More 2D crystals are produced, and the transfer is repeated again and again, until a desired stack is assembled. Conceptually, this is simple and requires only basic facilities such as a good optical microscope. In practice, the fabrication technique takes months to master. In addition to the standard clean-room procedures (cleaning, dissolving, resist spinning and so on), it is necessary to position different 2D crystals over each other with micro-metre accuracy. This is done under the microscope by using micromanipulators. The crystals must be put in soft contact without rubbing and, ideally no liquid or polymer should be allowed in contact with cleaved surfaces to minimize contamination. Thermal annealing in an inert atmosphere can often be helpful after adding each new layer. For transport measurements, 2D crystals are plasma etched into, for example, Hall bars with contacts evaporated as the final step.

Despite the dozens of steps involved, sophisticated multilayer structures can now be produced within a matter of days. Figure 3 shows two such examples. One is a van der Waals superlattice made from six alternating bilayers of graphene and hBN. This is the largest number of 2D crystals in a van der Waals heterostructure reported so far<sup>16</sup>. The most challenging design has probably been double-layer graphene devices<sup>18</sup> such as those shown in Fig. 3b, c. We emphasize that interfaces in these heterostructures are found to be clean and atomically sharp<sup>16,19</sup>, without the contaminating ‘goo’ that always covers 2D crystals even in high

vacuum (see the ‘Layered reality check’ section). **The reason for the clean interfaces is the van der Waals forces that attract adjacent crystals and effectively squeeze out trapped contaminants or force them into micro-metre-sized ‘bubbles’<sup>16</sup>.** This allows 10- $\mu\text{m}$ -scale devices that are effectively free from contamination. We also note that atomically sharp interfaces are in practice impossible to achieve by other techniques, including molecular beam epitaxy, because of island growth.

### Little evolutionary steps

Although the availability of various isolated 2D crystals had been recognized<sup>6</sup>, practical steps towards their van der Waals assembly were taken only after 2010. An important stimulus was the demonstration that hBN could serve as a high-quality substrate for graphene<sup>2</sup> (many other substrates, including pyrolytic hBN, were unsuccessfully tried before<sup>35,67</sup>). This led to rapid development of transfer procedures. The next logical step was encapsulation, where thin hBN crystals served not only as the substrate but also as a protective cover for graphene<sup>3</sup>. Encapsulation has proved its worth by enabling devices with consistently high quality that do not deteriorate under ambient conditions. The most commonly achieved mobility for graphene on hBN is  $\mu \approx 100,000 \text{ cm}^2 \text{ V}^{-1} \text{ s}^{-1}$  but up to  $500,000 \text{ cm}^2 \text{ V}^{-1} \text{ s}^{-1}$  can be reached at low temperature. Such high quality (as indicated by high mobility) can be witnessed directly as negative bend resistance and magnetic focusing<sup>3,36</sup> (Fig. 4a). These ballistic effects persist up to room temperature. The encapsulation also results in high spatial uniformity so that capacitors over  $100 \mu\text{m}^2$  in size exhibit quantum oscillations in magnetic fields  $B$  as low as 0.2 T (ref. 68).

The next evolutionary step has been ‘vertical’ devices in which few-layer-thick crystals of hBN,  $\text{MoS}_2$  or  $\text{WS}_2$  are used as tunnel barriers with graphene serving as one or both electrodes<sup>15,19</sup>. These devices require three to four transfers, but no plasma etching, to define their geometry. Although sensitive to charge inhomogeneity, vertical devices usually do not pose critical demands on  $\mu$ . The tunnelling heterostructures allow the demonstration of a new kind of electronic device: field-effect tunnelling transistors<sup>15</sup>. **In these, the tunnel current is controlled by changes in the electrode’s Fermi energy, which can be varied by gate voltage by as much as about 0.5 eV owing to the low density of states in monolayer graphene.** An increase in the Fermi energy effectively lowers the tunnel barrier, even if no bias is applied<sup>15</sup>. This is in contrast to the standard Fowler–Nordheim mechanism, which is based on tilting the top of the tunnel barrier by applied bias. The van der Waals tunnelling devices exhibit an on/off switching ratio of over  $10^6$  at room temperature<sup>15,19,69</sup>.

A higher level of complexity is presented by the graphene–hBN superlattice shown in Fig. 3a. It proves the concept that thin films of new 3D materials consisting of dozens of atomic layers are in principle possible by reassembly, as discussed in the ‘Dreamscape’ section. In the case of Fig. 3a, hBN bilayers serve as spacers whereas bilayer graphene (rather than its monolayer) was chosen to facilitate intercalation to reach a high density of states. Further efforts in making and investigating such multilayer structures are expected, given the interest generated by a large amount of literature on possible collective phenomena in graphene-based systems<sup>23–28,70–72</sup>.

The double-layer devices in Fig. 3 represent the state of the art for van der Waals heterostructures. They were designed to probe in-plane transport in the regime of the strongest possible electron–electron interaction between electrically isolated 2D systems<sup>18,73</sup>. The separation of the graphene layers can be as small as three hBN layers (about 1 nm)<sup>18</sup> but this still provides a sufficiently high potential barrier to suppress electron tunnelling. The layers continue to ‘feel’ each other strongly through Coulomb interactions. The 1-nm separation is much smaller than the in-plane distance between charge carriers in graphene, which is typically around 10 nm and nominally diverges near the neutrality point. This makes the interlayer separation the smallest spatial parameter in the problem. Therefore, the two electronic liquids in double-layer graphene effectively nest within the same plane, but can still be tuned and measured separately.

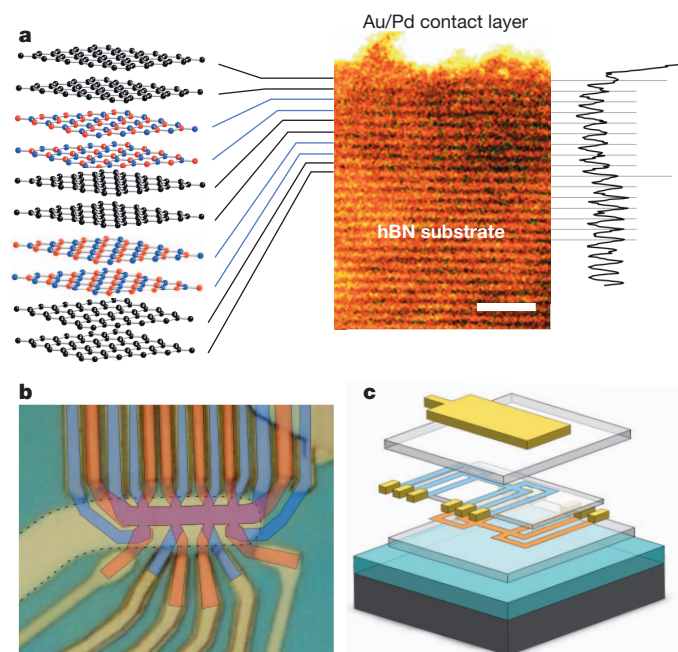


**Figure 3 | State-of-the-art van der Waals structures and devices.**

**a**, Graphene–hBN superlattice consisting of six stacked bilayers. On the right its cross-section and intensity profile as seen by scanning transmission electron microscopy are shown; on the left is a schematic view of the layer sequence. The topmost hBN bilayer is not visible, being merged with the metallic contact. Scale bar, 2 nm. (Adapted from ref. 16.) **b**, **c**, Double-layer graphene heterostructures<sup>18</sup>. An optical image of a working device (**b**) and its schematics in matching colours (**c**). Two graphene Hall bars are accurately aligned, separated by a trilayer hBN crystal and encapsulated between relatively thick hBN crystals (hBN is shown in **c** as semitransparent slabs). The entire heterostructure is placed on top of an oxidized Si wafer ( $\text{SiO}_2$  is in turquoise). The colours in **b** indicate the top (blue) and bottom (orange) Hall bars and their overlapping region (violet). The graphene areas are invisible in the final device image because of the top Au gate outlined by dashes. The scale is given by the width of the Hall bars, 1.5  $\mu\text{m}$ .

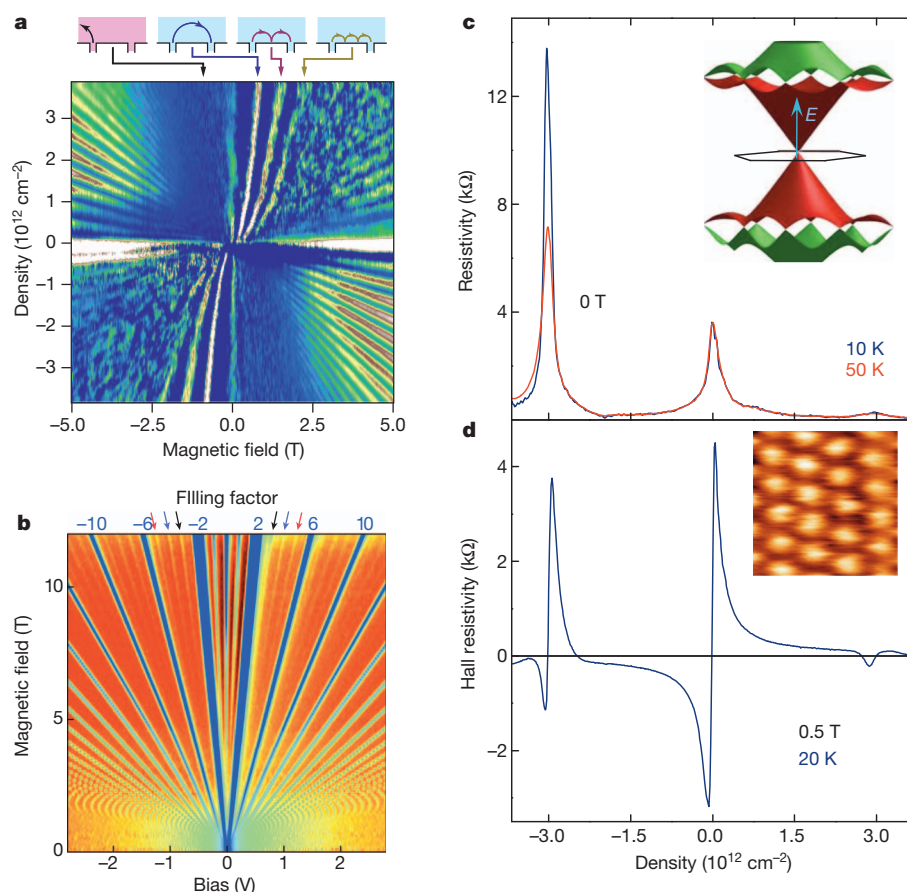


**Figure 4 | Early harvest in van der Waals fields.** **a**, Magnetic focusing in graphene on hBN. Pronounced resonances are observed if the size of a cyclotron orbit becomes commensurate with the distance between narrow graphene leads used as an injector and a detector (adapted from ref. 36). Bright colours show maxima in conductivity as a function of carrier density (positive and negative densities correspond to electrons and holes, respectively) and  $B$ . The upper panel illustrates the corresponding trajectories. **b**, Quantum capacitance of encapsulated graphene as a function of gate voltage and  $B$ . In this device, spin and valley degeneracies are lifted above 10 T. (Adapted from ref. 68.) **c**, **d**, Importance of crystallographic alignment. The standard Dirac-like spectrum is strongly reconstructed for graphene on hBN, and new Dirac cones appear in both valence and conduction bands (inset in **c**). This leads to pronounced peaks in resistivity (**c**) and the Hall effect changes sign (**d**). The inset in **d** shows the moiré patterns that lead to the spectral reconstruction. (Adapted from ref. 76.)

The ambition behind the double-layer heterostructures is to address many possible collective states, including Wigner crystallization, excitonic superfluidity, itinerant magnetism and so on. Such many-body phenomena have so far been the domain of low-temperature physics. In particular, Bose condensation of interlayer excitons has been reported at sub-Kelvin temperatures in double-layer semiconductor heterostructures, and Coulomb drag has been used as a way of detecting the condensate<sup>74,75</sup>. The hope was that double-layer graphene would allow a similar superfluid state but at much higher temperature<sup>27,28</sup> because the Coulomb energy of interlayer interaction can exceed 0.1 eV. The measurements<sup>18</sup> revealed many interesting and some unexpected features but no sign of superfluidity at zero magnetic field  $B$  so far. By analogy with the semiconductor heterostructures<sup>74,75</sup>, the regime of quantizing  $B$  remains the most promising for the observation of coherent electronic states, but this has not been investigated yet.

Another important step in the sophistication of van der Waals heterostructures was to include crystallographic alignment, which can be done with an accuracy of less than  $1^\circ$  (ref. 76). Although the interaction between stacked 2D crystals is relatively weak (around  $10 \text{ meV } \text{\AA}^{-2}$ ; ref. 77), electron orbitals still extend out of the plane and affect charge carriers in an adjacent 2D crystal. This influence results in moiré patterns that depend on the rotation angle between joining crystals and their lattice mismatch<sup>78–80</sup> (Fig. 4d). In the case of graphene on hBN, a periodic potential created by the hBN substrate results in additional Dirac cones at high electron and hole densities<sup>76,81</sup> (Fig. 4c). The superlattice effects are remarkably strong, such that the Hall effect changes its sign (Fig. 4d) and the new Dirac cones exhibit their own sets of Landau levels<sup>76,81</sup>. This is the best proof so far that interfacial contamination can be negligible and also shows that the electronic spectra of van der Waals heterostructures can be tuned by using moiré potentials. As another example of such bandgap engineering, one can consider the alignment of monolayers that have close lattice constants (for example,  $\text{MoS}_2$  and  $\text{WSe}_2$ ). The resulting van der Waals crystal is expected to exhibit optical and electronic properties distinct from its components<sup>82</sup>.

Many other types of van der Waals structure and device are expected to be demonstrated soon, initially using only a small number of 2D crystals. Among obvious objectives are various proximity effects. To this end, 2D crystals can be put on top of atomically flat crystals exhibiting magnetism, ferroelectricity, spin–orbit coupling and so on. **For example, graphene encapsulated in  $\text{WS}_2$  is likely to exhibit an induced spin–orbit interaction that should affect transport properties.**

### Handicraft on industrial scale

The growing interest in van der Waals heterostructures is not limited to new physics and materials science. There is also a massive potential for applications. Here we avoid early speculations because interest in van der Waals heterostructures is already justified if one considers them as a way of accelerating the development of the myriad applications offered by graphene itself. The recently demonstrated new graphene-based device architectures<sup>1,15,83</sup> provide straightforward examples.

Any industrial application will require a scalable approach to van der Waals assembly. To this end, significant efforts have been reported to grow graphene, 2D hBN and 2D  $\text{MoS}_2$  epitaxially on top of each other<sup>10,84–88</sup>. However, it is a daunting task to find the right conditions for so-called van der Waals epitaxy<sup>89</sup> because the weak interlayer interaction generally favours island growth rather than that of continuous monolayers. Another scalable approach is layer-by-layer deposition from 2D-crystal suspensions by using Langmuir–Blodgett or similar techniques<sup>8,90</sup>. One can also mix suspensions of different 2D crystals and then make layer-by-layer laminates, relying on self-organizational assembly (flocculation)<sup>11</sup>. Unfortunately, micrometre-sized crystallites in suspensions cannot provide large continuous layers, and this would limit possible applications for such van der Waals laminates. At present, they are being considered for use as designer ultrathin dielectrics<sup>8</sup>, selectively permeable membranes<sup>91</sup> and composite materials<sup>92</sup>.

At the time of writing, the most feasible approach to industrial-scale production of van der Waals heterostructures seems to involve growing



individual monolayers on catalytic substrates, then isolating and stacking these 2D sheets. This route has already been proved to be scalable<sup>61,64</sup>. If a particular heterostructure attracts sufficient interest in terms of applications, it seems inevitable that its production can be scaled up by trying a variety of available approaches.

## Long live graphene

After many years of intensive effort, graphene research should logically have reached a mature stage. However, the possibility of combining graphene with other 2D crystals has expanded this field dramatically, well beyond simple graphene or 2D MoS<sub>2</sub>. The interest in van der Waals heterostructures is growing as quickly as interest in graphene did a few years ago. As the technology of making van der Waals heterostructures moves from its humble beginnings, increasingly sophisticated devices and materials should become available to more and more research groups. This is likely to cause a snowball effect because, with so many 2D crystals, sequences and parameters to consider, the choice of possible van der Waals structures is limited only by our imagination. Even with the 2D components that have been shown to be stable, it will take time and effort to explore the huge parameter space. The decades of research on semiconductor heterostructures and devices may serve as a guide to judge the probable longevity of research on van der Waals materials, beyond simple graphene.

Received 1 April; accepted 12 June 2013.

- Novoselov, K. S. *et al.* A roadmap for graphene. *Nature* **490**, 192–200 (2012).
- Dean, C. R. *et al.* Boron nitride substrates for high-quality graphene electronics. *Nature Nanotechnol.* **5**, 722–726 (2010).
- This paper attracted attention to hBN as a substrate and initiated the development of transfer techniques essential for the van der Waals reassembly.**
- Mayorov, A. S. *et al.* Micrometer-scale ballistic transport in encapsulated graphene at room temperature. *Nano Lett.* **11**, 2396–2399 (2011).
- Mayorov, A. S. *et al.* How close can one approach the Dirac point in graphene experimentally? *Nano Lett.* **12**, 4629–4634 (2012).
- Bao, W. *et al.* Evidence for a spontaneous gapped state in ultraclean bilayer graphene. *Proc. Natl Acad. Sci. USA* **109**, 10802–10805 (2012).
- Novoselov, K. S. *et al.* Two-dimensional atomic crystals. *Proc. Natl Acad. Sci. USA* **102**, 10451–10453 (2005).
- This was the first paper to demonstrate the electric field effect and study electron transport in 2D crystals other than graphene.**
- Mas-Ballester, R., Gómez-Navarro, C., Gómez-Herrero, J. & Zamora, F. 2D materials: to graphene and beyond. *Nanoscale* **3**, 20–30 (2011).
- Osada, M. & Sasaki, T. Two-dimensional dielectric nanosheets: novel nanoelectronics from nanocrystal building blocks. *Adv. Mater.* **24**, 210–228 (2012).
- Wang, Q. H., Kalantar-Zadeh, K., Kis, A., Coleman, J. N. & Strano, M. S. Electronics and optoelectronics of two-dimensional transition metal dichalcogenides. *Nature Nanotechnol.* **7**, 699–712 (2012).
- Xu, M., Lian, T., Shi, M. & Chen, H. Graphene-like two-dimensional materials. *Chem. Rev.* **113**, 3766–3798 (2013).
- We recommend this review for initial acquaintance with 2D materials other than graphene.**
- Butler, S. Z. *et al.* Progress, challenges, and opportunities in two-dimensional materials beyond graphene. *ACS Nano* **7**, 2898–2926 (2013).
- Radisavljevic, B., Radenovic, A., Brivio, J., Giacometti, V. & Kis, A. Single-layer MoS<sub>2</sub> transistors. *Nature Nanotechnol.* **6**, 147–150 (2011).
- The paper attracted critical attention to electron transport in MoS<sub>2</sub> monolayers.**
- Fuhrer, M. S. & Hone, J. Measurement of mobility in dual-gated MoS<sub>2</sub> transistors. *Nature Nanotechnol.* **8**, 146–147 (2013).
- Ponomarenko, L. A. *et al.* Tunable metal-insulator transition in double-layer graphene heterostructures. *Nature Phys.* **7**, 958–961 (2011).
- This is the first demonstration of multilayer van der Waals heterostructures, beyond using hBN, mica and so on as a substrate.**
- Britnell, L. *et al.* Field-effect tunneling transistor based on vertical graphene heterostructures. *Science* **335**, 947–950 (2012).
- Haigh, S. J. *et al.* Cross-sectional imaging of individual layers and buried interfaces of graphene-based heterostructures and superlattices. *Nature Mater.* **11**, 764–767 (2012).
- The paper proves the concept of complex heterostructures, including manually assembled van der Waals superlattices, and shows that their interfaces can be atomically sharp and clean.**
- Dean, C. R. *et al.* Graphene based heterostructures. *Solid State Commun.* **152**, 1275–1282 (2012).
- Gorbachev, R. V. *et al.* Strong Coulomb drag and broken symmetry in double-layer graphene. *Nature Phys.* **8**, 896–901 (2012).
- Georgiou, T. *et al.* Vertical field-effect transistor based on graphene–WS<sub>2</sub> heterostructures for flexible and transparent electronics. *Nature Nanotechnol.* **8**, 100–103 (2013).
- Kastner, M. A., Birgeneau, R. J., Shirane, G. & Endoh, Y. Magnetic, transport, and optical properties of monolayer copper oxides. *Rev. Mod. Phys.* **70**, 897–928 (1998).
- Orenstein, J. & Millis, A. J. Advances in the physics of high-temperature superconductivity. *Science* **288**, 468–474 (2000).
- Weller, T. E., Ellerby, M., Saxena, S. S., Smith, R. P. & Skipper, N. T. Superconductivity in the intercalated graphite compounds C<sub>6</sub>Yb and C<sub>6</sub>Ca. *Nature Phys.* **1**, 39–41 (2005).
- Profeta, G., Calandra, M. & Mauri, F. Phonon-mediated superconductivity in graphene by lithium deposition. *Nature Phys.* **8**, 131–134 (2012).
- Nandkishore, R., Levitov, L. S. & Chubukov, A. V. Chiral superconductivity from repulsive interactions in doped graphene. *Nature Phys.* **8**, 158–163 (2012).
- Savini, G., Ferrari, A. C. & Giustino, F. First-principles prediction of doped graphene as a high-temperature electron-phonon superconductor. *Phys. Rev. Lett.* **105**, 037002 (2010).
- Guinea, F. & Uchoa, B. Odd-momentum pairing and superconductivity in vertical graphene heterostructures. *Phys. Rev. B* **86**, 134521 (2012).
- Min, H., Bistrizter, R., Su, J. J. & MacDonald, A. H. Room-temperature superfluidity in graphene bilayers. *Phys. Rev. B* **78**, 121401 (2008).
- Perali, A., Neilson, D. & Hamilton, A. R. High-temperature superfluidity in double-bilayer graphene. *Phys. Rev. Lett.* **110**, 146803 (2013).
- Geim, A. K. Random walk to graphene. *Rev. Mod. Phys.* **83**, 851–862 (2011).
- Liu, L. *et al.* Graphene oxidation: thickness-dependent etching and strong chemical doping. *Nano Lett.* **8**, 1965–1970 (2008).
- Elias, D. C. *et al.* Control of graphene's properties by reversible hydrogenation: evidence for graphane. *Science* **323**, 610–613 (2009).
- Ross, S. & Sussman, A. Surface oxidation of molybdenum disulfide. *J. Phys. Chem.* **59**, 889–892 (1955).
- Vogt, P. *et al.* Silicene: compelling experimental evidence for graphenelike two-dimensional silicon. *Phys. Rev. Lett.* **108**, 155501 (2012).
- Fleurence, A. *et al.* Experimental evidence for epitaxial silicene on diboride thin films. *Phys. Rev. Lett.* **108**, 245501 (2012).
- Lui, C. H., Liu, L., Mak, K. F., Flynn, G. W. & Heinz, T. F. Ultraflat graphene. *Nature* **462**, 339–341 (2009).
- Taychatanapat, T., Watanabe, K., Taniguchi, T. & Jarillo-Herrero, P. Electrically tunable transverse magnetic focusing in graphene. *Nature Phys.* **9**, 225–229 (2013).
- Watanabe, K., Taniguchi, T. & Kanda, H. Direct-bandgap properties and evidence for ultraviolet lasing of hexagonal boron nitride single crystal. *Nature Mater.* **3**, 404–409 (2004).
- Zomer, P. J., Dash, S. P., Tombros, N. & van Wees, B. J. A transfer technique for high mobility graphene devices on commercially available hexagonal boron nitride. *Appl. Phys. Lett.* **99**, 232104 (2011).
- Meric, I. *et al.* Graphene field-effect transistors based on boron nitride gate dielectrics. *Tech. Digest Int. Electron Devices Meet. 2010 IEEE Int.* **10**, 556–559, doi:10.1109/IEDM.2010.5703419 (2010).
- Lee, G. H. *et al.* Electron tunneling through atomically flat and ultrathin hexagonal boron nitride. *Appl. Phys. Lett.* **99**, 243114 (2011).
- Britnell, L. *et al.* Electron tunneling through ultrathin boron nitride crystalline barriers. *Nano Lett.* **12**, 1707–1710 (2012).
- Gordon, R. A., Yang, D., Crozier, E. D., Jiang, D. T. & Frindt, R. F. Structures of exfoliated single layers of WS<sub>2</sub>, MoS<sub>2</sub>, and MoSe<sub>2</sub> in aqueous suspension. *Phys. Rev. B* **65**, 125407 (2002).
- Splendiani, A. *et al.* Emerging photoluminescence in monolayer MoS<sub>2</sub>. *Nano Lett.* **10**, 1271–1275 (2010).
- Mak, K. F., Lee, C., Hone, J., Shan, J. & Heinz, T. F. Atomically thin MoS<sub>2</sub>: a new direct-gap semiconductor. *Phys. Rev. Lett.* **105**, 136805 (2010).
- Zeng, H., Dai, J., Yao, W., Xiao, D. & Cui, X. Valley polarization in MoS<sub>2</sub> monolayers by optical pumping. *Nature Nanotechnol.* **7**, 490–493 (2012).
- Mak, K. F., He, K., Shan, J. & Heinz, T. F. Control of valley polarization in monolayer MoS<sub>2</sub> by optical helicity. *Nature Nanotechnol.* **7**, 494–498 (2012).
- Fang, H. *et al.* High-performance single layered WS<sub>2</sub> p-FETs with chemically doped contacts. *Nano Lett.* **12**, 3788–3792 (2012).
- Zhao, W. *et al.* Evolution of electronic structure in atomically thin sheets of WS<sub>2</sub> and WSe<sub>2</sub>. *ACS Nano* **7**, 791–797 (2013).
- Tonndorf, P. *et al.* Photoluminescence emission and Raman response of monolayer MoS<sub>2</sub>, MoSe<sub>2</sub>, and WSe<sub>2</sub>. *Opt. Express* **21**, 4908–4916 (2013).
- Nair, R. R. *et al.* Fluorographene: a two-dimensional counterpart of Teflon. *Small* **6**, 2877–2884 (2010).
- Bianco, E. *et al.* Stability and exfoliation of germanene: a germanium graphene analogue. *ACS Nano* **7**, 4414–4421 (2013).
- Park, S. & Ruoff, R. S. Chemical methods for the production of graphenes. *Nature Nanotechnol.* **4**, 217–224 (2009).
- Jin, Z., Yao, J., Kittrell, C. & Tour, J. M. Large-scale growth and characterizations of nitrogen-doped monolayer graphene sheets. *ACS Nano* **5**, 4112–4117 (2011).
- Ci, L. *et al.* Atomic layers of hybridized boron nitride and graphene domains. *Nature Mater.* **9**, 430–435 (2010).
- Gamble, F. R. *et al.* Intercalation complexes of Lewis bases and layered sulfides: a large class of new superconductors. *Science* **174**, 493–497 (1971).
- Coleman, J. N. *et al.* Two-dimensional nanosheets produced by liquid exfoliation of layered materials. *Science* **331**, 568–571 (2011).
- Addou, R., Dahal, A. & Batzill, M. Growth of a two-dimensional dielectric monolayer on quasi-freestanding graphene. *Nature Nanotechnol.* **8**, 41–45 (2013).
- Tusche, C., Meyerheim, H. L. & Kirschner, J. Observation of depolarized ZnO(0001) monolayers: formation of unreconstructed planar sheets. *Phys. Rev. Lett.* **99**, 026102 (2007).

59. Reina, A. *et al.* Large area, few-layer graphene films on arbitrary substrates by chemical vapor deposition. *Nano Lett.* **9**, 30–35 (2009).
60. Li, X. *et al.* Large-area synthesis of high-quality and uniform graphene films on copper foils. *Science* **324**, 1312–1314 (2009).
61. Bae, S. *et al.* Roll-to-roll production of 30-inch graphene films for transparent electrodes. *Nature Nanotechnol.* **5**, 574–578 (2010).
62. Song, L. *et al.* Large scale growth and characterization of atomic hexagonal boron nitride layers. *Nano Lett.* **10**, 3209–3215 (2010).
63. Kim, K. K. *et al.* Synthesis of monolayer hexagonal boron nitride on Cu foil using chemical vapor deposition. *Nano Lett.* **12**, 161–166 (2012).
64. Bresnahan, M. S. *et al.* Integration of hexagonal boron nitride with quasi-freestanding epitaxial graphene: toward wafer-scale, high-performance devices. *ACS Nano* **6**, 5234–5241 (2012).
65. Bertolazzi, S., Krasnozhan, D. & Kis, A. Nonvolatile memory cells based on MoS<sub>2</sub>/graphene heterostructures. *ACS Nano* **7**, 3246–3252 (2013).
66. Hunt, B. *et al.* Massive Dirac fermions and Hofstadter butterfly in a van der Waals heterostructure. *Science* **340**, 1427–1430 (2013).
67. Ponomarenko, L. A. *et al.* Effect of a high-kappa environment on charge carrier mobility in graphene. *Phys. Rev. Lett.* **102**, 206603 (2009).
68. Yu, G. L. *et al.* Interaction phenomena in graphene seen through quantum capacitance. *Proc. Natl Acad. Sci. USA* **110**, 3282–3286 (2013).
69. Yang, H. *et al.* Graphene barristor, a triode device with a gate-controlled Schottky barrier. *Science* **336**, 1140–1143 (2012).
70. Kotov, V. N., Pereira, V. M., Castro Neto, A. H. & Guinea, F. Electron–electron interactions in graphene: current status and perspectives. *Rev. Mod. Phys.* **84**, 1067–1125 (2012).
71. Das Sarma, S., Adam, S., Hwang, E. H. & Rossi, E. Electronic transport in two dimensional graphene. *Rev. Mod. Phys.* **83**, 407–470 (2011).
72. McChesney, J. L. *et al.* Extended van Hove singularity and superconducting instability in doped graphene. *Phys. Rev. Lett.* **104**, 136803 (2010).
73. Tutuc, E. & Kim, S. Magnetotransport and Coulomb drag in graphene double layers. *Solid State Commun.* **15**, 1283–1288 (2012).
74. Eisenstein, J. P. & MacDonald, A. H. Bose–Einstein condensation of excitons in bilayer electron systems. *Nature* **432**, 691–694 (2004).
75. Nandi, D., Finck, A. D. K., Eisenstein, J. P., Pfeiffer, L. N. & West, K. W. Exciton condensation and perfect Coulomb drag. *Nature* **488**, 481–484 (2012).
76. Ponomarenko, L. A. *et al.* Cloning of Dirac fermions in graphene superlattices. *Nature* **497**, 594–597 (2013).
77. Björkman, T., Gulans, A., Krashennnikov, A. V. & Nieminen, R. M. van der Waals bonding in layered compounds from advanced density-functional first-principles calculations. *Phys. Rev. Lett.* **108**, 235502 (2012).
78. Li, G. *et al.* Observation of Van Hove singularities in twisted graphene layers. *Nature Phys.* **6**, 109–113 (2010).
79. Decker, R. *et al.* Local electronic properties of graphene on a BN substrate via scanning tunneling microscopy. *Nano Lett.* **11**, 2291–2295 (2011).
80. Yankowitz, M. *et al.* Emergence of superlattice Dirac points in graphene on hexagonal boron nitride. *Nature Phys.* **8**, 382–386 (2012).
81. Dean, C. R. *et al.* Hofstadter's butterfly and fractal quantum Hall effect in moiré superlattices. *Nature* **497**, 598–602 (2013).
82. Kośmider, K. & Fernández-Rossier, J. Electronic properties of the MoS<sub>2</sub>-WS<sub>2</sub> heterojunction. *Phys. Rev. B* **87**, 075451 (2013).
83. Kim, K., Choi, J. Y., Kim, T., Cho, S. H. & Chung, H. J. A role for graphene in silicon-based semiconductor devices. *Nature* **479**, 338–344 (2011).
84. Tanaka, T., Ito, A., Tajiima, A., Rokuta, E. & Oshima, C. Heteroepitaxial film of monolayer graphene/monolayer h-BN on Ni(111). *Surf. Rev. Lett.* **10**, 721–726 (2003).
85. Yan, Z. *et al.* Growth of bilayer graphene on insulating substrates. *ACS Nano* **5**, 8187–8192 (2011).
86. Liu, Z. *et al.* Direct growth of graphene/hexagonal boron nitride stacked layers. *Nano Lett.* **11**, 2032–2037 (2011).
87. Garcia, J. M. *et al.* Graphene growth on h-BN by molecular beam epitaxy. *Solid State Commun.* **152**, 975–978 (2012).
88. Shi, Y. *et al.* Van der Waals epitaxy of MoS<sub>2</sub> layers using graphene as growth templates. *Nano Lett.* **12**, 2784–2791 (2012).
89. Koma, A. Van der Waals epitaxy—a new epitaxial growth method for a highly lattice-mismatched system. *Thin Solid Films* **216**, 72–76 (1992).
90. Ariga, K., Ji, Q., Hill, J. P., Bando, Y. & Aono, M. Forming nanomaterials as layered functional structures toward materials nanoarchitectonics. *NPG Asia Mater.* **4**, e17, doi:10.1038/am.2012.30 (2012).
91. Nair, R. R., Wu, H. A., Jayaram, P. N., Grigorieva, I. V. & Geim, A. K. Unimpeded permeation of water through helium-leak-tight graphene-based membranes. *Science* **335**, 442–444 (2012).
92. Young, R. J., Kinloch, I. A., Gong, L. & Novoselov, K. S. The mechanics of graphene nanocomposites: a review. *Compos. Sci. Technol.* **72**, 1459–1476 (2012).

**Acknowledgements** We thank all participants of the Friday Graphene Seminar in Manchester for discussions, and R. Gorbachev and J. Chapman for help with the figures. This work was supported by the Royal Society, the European Research Council, the Körber Foundation, the Office of Naval Research and the Air Force Office of Scientific Research.

**Author Contributions** A.K.G. wrote a draft that was scrutinized and improved by both authors.

**Author Information** Reprints and permissions information is available at [www.nature.com/reprints](http://www.nature.com/reprints). The authors declare no competing financial interests. Readers are welcome to comment on the online version of the paper. Correspondence should be addressed to I.V.G. ([irina.grigorieva@man.ac.uk](mailto:irina.grigorieva@man.ac.uk)).